

Original Paper

# Pulse Position Modulation with Flexible Dimming Support for Visible Light Communication

Poompat Saengudomlert and Karel L. Sterckx\*

*Bangkok University-Center of Research in Optoelectronics, Communications, and Computational Systems (BU-CROCCS), Thailand*

---

## ABSTRACT

Data transmissions based on Pulse Position Modulation (PPM) and its variants are considered for indoor localization using Visible Light Communication (VLC). To support different illumination levels for pleasant environments and for energy savings when background light is sufficient, light dimming is required. While there are existing PPM based modulation schemes with dimming support, those relying on adjusting the Direct Current (DC) bias or the pulse width suffer from low Signal-to-Noise Ratios (SNRs) at low illumination levels. Other schemes require signalling overheads or high computational complexities in encoding and decoding. These schemes are not suitable for short data transmissions in indoor localization systems with low-complexity mobile receivers. This work proposes a PPM based modulation scheme that supports dimming without signalling overhead and high-complexity encoding/decoding for dimming adjustment. The proposed scheme uses time division between PPM and Inverse PPM (IPPM), with dimming adjusted through varying the time fraction between PPM and IPPM. For each PPM/IPPM data symbol, pulse positions can be mapped to a point in a signal constellation, with one constellation for one dimming level. To provide for flexible dimming in which a transmitter need not inform a receiver which constellation is used (i.e., no signalling

---

\*Corresponding author: Karel L. Sterckx, [karel.s@bu.ac.th](mailto:karel.s@bu.ac.th).

overhead), detection of data bits based on multiple signal constellations is investigated. In particular, each data symbol is mapped to a cluster of signal points instead of a single point. The conventional minimum-distance detection is still optimal, though the corresponding bit error rate (BER) depends on the minimum distance between signal clusters instead of between signal points. Finally, for BER improvements, detection based on successive data symbols is investigated.

---

*Keywords:* visible light communication, light dimming, pulse position modulation, signal constellation, minimum-distance detection, symbol error rate.

## 1 Introduction

Visible Light Communication (VLC) has been investigated as an alternative or complimentary technology to wireless communications using radio frequencies (RFs) [3, 8, 15, 16]. Unlicensed frequency bands, low-cost hardware, and energy efficiency from using Light Emitting Diode (LED) lamps for both illumination and data transmissions are among the advantages offered by VLC.

In addition to supporting data transmissions, VLC has also been considered for indoor localization [1, 5]. The coverage area of each LED lamp is limited (typically a few meters) and is referred to as an optical attocell [15]. For a number of indoor object tracking applications, knowing in which attocell the object of interest is located is sufficiently accurate. Examples of such applications include wheelchair tracking in a hospital and cart tracking in an airport. In such scenarios, location identification numbers can be transmitted from LED lamps, providing location information to mobile VLC receivers.

Light dimming is an important feature of VLC systems for pleasant illumination atmospheres as well as for energy savings when background light is sufficient. Various signal modulation schemes with dimming support have been investigated for single-carrier as well as multi-carrier systems [14, 24, 25]. Since this work focuses on data transmissions for VLC-based indoor localization, which does not require high transmission rates, only single-carrier modulation schemes are considered. Existing single-carrier modulation schemes with dimming support for VLC are next introduced together with their drawbacks for the purpose of indoor localization.

Most of the proposed dimming schemes for VLC with single-carrier modulation utilize Pulse Position Modulation (PPM) and its variants [4, 6, 10, 12, 13, 17, 21]. Other proposed schemes rely on varying the Direct Current (DC) bias added to data signals [14], and varying the number of activated LEDs in a panel [11]. Due to limited signal dynamic ranges for LED modulation, varying

the DC bias can lead to significant signal distortion at a high illumination level. On the other hand, at a low illumination level, activating only a subset of LEDs in a transmitter leads to a low signal power, and hence a low Signal-to-Noise Ratio (SNR) and a high Bit Error Rate (BER) at a receiver.

In Variable PPM (VPPM) supported by the IEEE 802.15.17 standard [10], Pulse Width Modulation (PWM) and binary PPM are combined to support light dimming. Hardware demonstrations of VPPM have been reported in [12, 17]. In [23], a combination of delta signal modulation and PWM has been investigated for the purpose of dimming control. However, at a low illumination level, narrow pulse widths associated with these PWM based schemes can lead to a low signal power and a high BER at a receiver.

Light dimming based on PPM using fixed-width pulses has been investigated in [4, 6, 13, 21]. In [13], the authors investigated the throughput and BER performances of  $M$ -ary PPM ( $M$ -PPM) and  $M$ -ary Inverted PPM ( $M$ -IPPM) for different values of  $M$ . In [21], the use of multi-pulse PPM, in which positions of multiple pulses in each symbol period represent data bits, was investigated and shown to improve the BER performances. By varying the number of pulses in each symbol period, different dimming levels can be provided. In addition, a connection was made between dimming support using multi-pulse PPM and the design of binary codes with fixed Hamming weights known as constant-weight codes [2]. In both [13] and [21], each receiver is assumed to know the modulation scheme and can accordingly perform detection of data bits. For short data packet transmissions for indoor localization, the amount of signalling required for a transmitter to inform a receiver about the modulation scheme will create significant transmission overheads.

In [4], a combination of  $M$ -PPM and  $M$ -IPPM is used for dimming control through the proposed coding and decoding algorithms for different dimming levels. In [6], the use of shaped polar codes for dimming control is proposed and investigated. While these dimming controls have been successfully demonstrated, they require much higher computational complexities compared to traditional  $M$ -PPM or  $M$ -IPPM and are not suitable for low-complexity mobile receivers in indoor localization.

In [22], the authors considered ASCII character transmissions in which each character is represented by two binary codewords, one for low and the other for high illumination levels. These codewords are transmitted using binary Pulse Amplitude Modulation (PAM) according to the Universal Asynchronous Receiver and Transmitter (UART) protocol. Since the illumination level varies with the transmitted characters, dimming is controlled in real time by continuously adjusting the proportion of low-illumination and high-illumination codewords used at the transmitter. This adaptive mechanism requires additional computational complexity at a transmitter, which can be avoided in indoor localization systems in which each LED lamp transmits its location number repeatedly.

In summary, the existing PPM based modulation schemes with dimming control are not suitable for short data packet transmissions in VLC based indoor localization systems. In particular, those relying on adjusting the DC bias or the pulse width suffer from low SNRs at low illumination levels. Others require significant signalling overheads or high computational complexities in encoding and decoding for dimming control. This work proposes a PPM based modulation scheme that uses fixed-width pulses without DC biasing, does not require signalling overheads, and does not employ complicated encoding and decoding. To do so, the multi-codeword concept in [22] is extended in this work for general data bit transmissions. Unlike [22], in the proposed scheme, the dimming level is data independent and hence the adaptive mechanism at a transmitter is no longer required.

In short, the proposed modulation scheme utilizes time division between  $M$ -PPM and  $M$ -IPPM to create a combined modulation scheme with the dimming level set through the time fraction between  $M$ -PPM and  $M$ -IPPM. For flexibility, LED transmitters in different locations may use different modulation schemes based on the desired dimming levels, e.g., lower illumination levels in locations with stronger background light. In addition, a transmitter may adjust the modulation scheme at any time without informing any receiver about the selected modulation scheme. In such scenarios, a moving receiver will receive data from different LED transmitters over time, with possibly different modulation schemes. A receiver therefore needs to detect data bits without knowing the selected modulation scheme.

The specific technical contributions of this work are as follows. First, using distinct PPM-based modulation schemes, or equivalently different signal constellations, for different dimming levels is described. With pulse positions for each data symbol mapped to a point in a signal constellation, each dimming level is associated with one signal constellation. The problem of selecting signal constellations for different dimming levels is formulated as an Integer Linear Programming (ILP) problem. Note that this approach of dimming was partly presented during an international conference in [20]. Then, an alternative dimming technique using time division between PPM and IPPM is proposed to offer a more flexible range of dimming levels with comparable or better BER performances. Finally, for further BER improvement, detection of successive data symbols with possibly different modulation schemes is investigated.

Section 2 presents the VLC system model used in the investigation. The use of distinct modulation schemes for different dimming levels is discussed in Section 3. An alternative dimming approach using time division between PPM and IPPM is proposed together with its BER analysis in Section 4. For further BER improvement, Section 5 considers detection of successive data symbols. Finally, a conclusion is made in Section 6.

## 2 System Model

Consider an indoor localization system based on VLC, as illustrated in Figure 1. To provide location information, LED lamps installed at different locations repeatedly transmit their location identification numbers. Assume that signal modulation is based on PPM and its variants. By using possibly different modulation schemes, different LED lamps can be independently dimmed while transmitting their location numbers. Assume that an object to be tracked, e.g., a hospital wheelchair, has a mobile VLC receiver that consists of a photodiode (PD), a signal amplifier circuit, and a demodulator that retrieves the location number from the received signal.

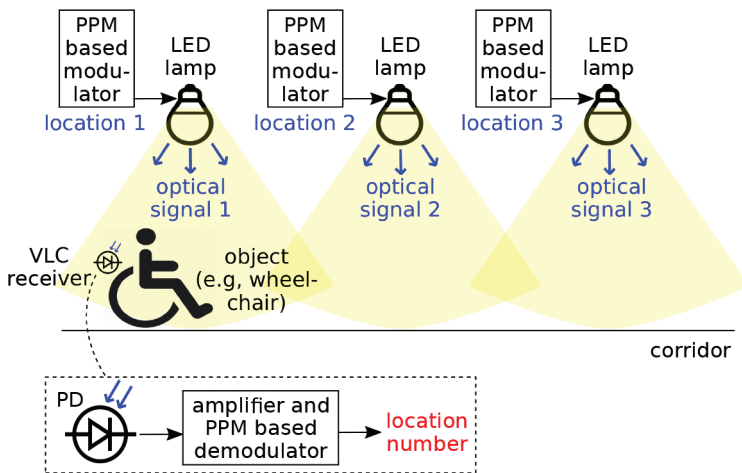


Figure 1: VLC based indoor localization system for object tracking.

Data transmissions via LED lamps in VLC systems rely on Intensity Modulation with Direct Detection (IM/DD) [3, 8]. For IM/DD, a data signal is used to drive the electrical current through an LED lamp, resulting in the transmit optical power and the illumination level that are proportional to the data signal. Hence, the average illumination level is proportional to the average data signal. At the receiver, the receive optical power is detected by a receiver's PD and converted back to a data signal.

Figure 2 shows components of a VLC transmitter in Figure 1. The location number associated with the transmitter is converted to data bits, which are mapped to a PPM symbol represented as a signal point in a signal constellation. The PPM signal point is then used to modulate pulses to generate a PPM signal, which is an input to an LED driver circuit. The drive current then determines the intensity of the emitted light, which varies according to the PPM signal. As mentioned above, the average PPM signal value determines

the illumination level. When the pulse period is sufficiently short, e.g., 1 ms, light flickering observable to human eyes is avoided.

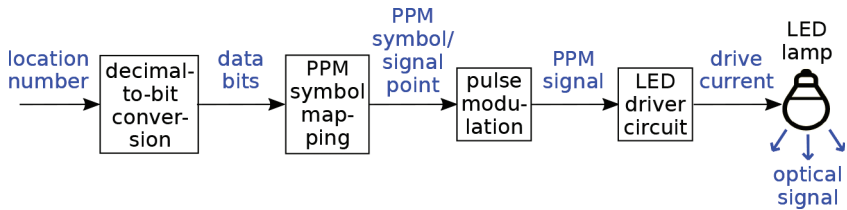


Figure 2: Details of a VLC transmitter in Figure 1.

Figure 3 shows components of a VLC receiver in Figure 1. The PD converts the light intensity of the received optical signal to a photocurrent, which is then amplified using a transimpedance amplifier to obtain a PPM voltage signal. The PPM signal is passed through a matched filter for noise reduction and then sampled at the rate of 1 sample per PPM timeslot to obtain a PPM signal point, or equivalently a PPM symbol, using the minimum-distance decision rule. Finally, the PPM symbol is demapped to obtain data bits which then yields the decimal location number.

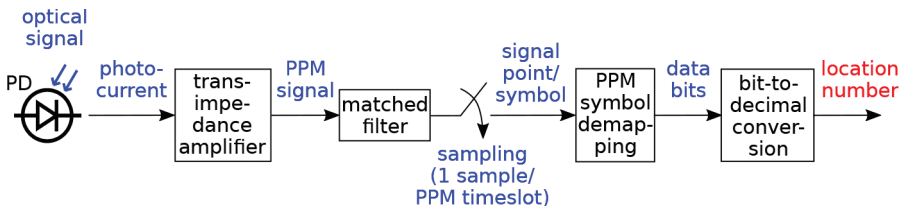


Figure 3: Details of a VLC receiver in Figure 1.

Let  $M$  be the number of timeslots in each PPM symbol period. For each  $M$ -PPM symbol, only one out of  $M$  timeslots contains a pulse, as illustrated in Figure 4 for  $M = 4$ . The corresponding illumination percentage is  $1/M \times 100\%$ , where 100% corresponds to having a pulse in all timeslots (with no data transmission). On the other hand, for each  $M$ -IPPM symbol, only one out of  $M$  timeslots does not contain a pulse, as illustrated in Figure 4. Its illumination percentage is  $(M - 1)/M \times 100\%$ . For both  $M$ -PPM and  $M$ -IPPM, the bit rate is  $\log_2 M$  bit/symbol.

In multi-pulse  $M$ -PPM,  $K$  out of  $M$  timeslots contain a pulse, where  $K \in \{2, \dots, M - 1\}$ . Figure 4 illustrates the case of  $M = 4$  and  $K = 2$ . Its illumination percentage is  $K/M \times 100\%$ . Since there are  $\binom{M}{K}$  ways to place  $K$  pulses in  $M$  timeslots, the bit rate can be up to  $\log_2 \binom{M}{K}$  bit/symbol. However,  $M$  out of  $\binom{M}{K}$  possible signals may be selected to keep the same bit rate as

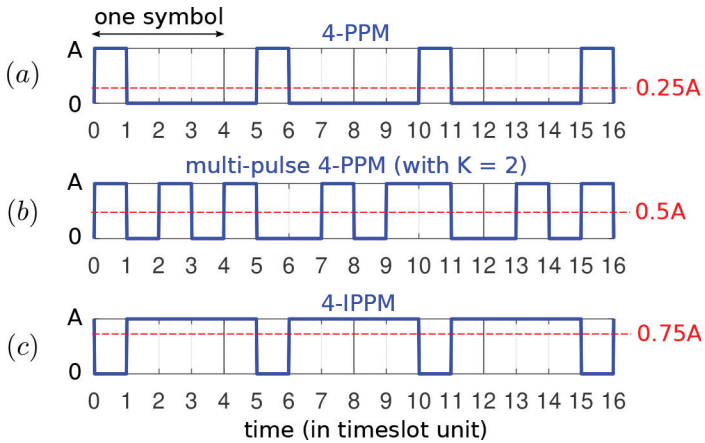


Figure 4: Example  $M$ -PPM,  $M$ -IPPM, and multi-pulse  $M$ -PPM signals for  $M = 4$ , with the average signal values, shown as red dashed lines, equal to (a)  $0.25A$ , (b)  $0.5A$ , and (c)  $0.75A$ . Each example signal contains 4 data symbols for bits 00, 01, 10, and 11, respectively. Each pulse signal is rectangular with amplitude  $A$ .

Table 1: Signal constellations for 4-PPM, multi-pulse 4-PPM (using  $K = 2$  pulses per symbol), and 4-IPPM.

PPM scheme	Data bits			
	00	01	10	11
4-PPM	$(A, 0, 0, 0)$	$(0, A, 0, 0)$	$(0, 0, A, 0)$	$(0, 0, 0, A)$
Multi-pulse 4-PPM	$(A, 0, A, 0)$	$(A, 0, 0, A)$	$(0, A, A, 0)$	$(0, A, 0, A)$
4-IPPM	$(0, A, A, A)$	$(A, 0, A, A)$	$(A, A, 0, A)$	$(A, A, A, 0)$

$M$ -PPM and  $M$ -IPPM. Figure 4 illustrates this approach for  $M = 4$  and  $K = 2$ , where only 4 out of  $\binom{4}{2} = 6$  possible signals are used.

A mobile receiver detects its location from the closest LED lamp above it. Assume that timeslot synchronization is performed based on timing information observed from level transitions in the received signal at timeslot boundaries. Assume that symbol synchronization is performed based on the use of synchronization waveforms transmitted before data symbols. In addition, assume the use of Automatic Gain Control (AGC) such that, in a noiseless received signal, the high signal level is equal to  $A$  while the low signal level is equal to 0.

Since the receiver does not know which modulation scheme is used, it detects data bits by considering all possible signal points used by the transmitter. Table 1 shows signal constellations associated with 4-PPM, multi-pulse 4-PPM, and 4-IPPM for 25%, 50%, and 75% of illumination, respectively.

Assume that transmitted signals are subject to Additive White Gaussian Noise (AWGN) with a two-sided Power Spectral Density (PSD) equal to  $N_0/2$ . Moreover, assume that LED lamps are sufficiently separated and their coverages do not significantly overlapped, making signal interference between adjacent LED lamps negligible compared to AWGN. With AWGN, optimal detection of data bits is based on the minimum-distance decision rule [7].

In particular, denote the received signal vector for a data symbol of interest by  $\mathbf{r} = (r_1, \dots, r_M)$ . Let  $\mathbf{s}_1, \dots, \mathbf{s}_N$  denote the signal points from all constellations, where  $N$  is the total number of points. Note that, for the signal points in Table 1,  $M = 4$  and  $N = 12$ . The minimum-distance decision rule is to choose the signal point index  $i^*$  such that

$$i^* = \arg \min_{i \in \{1, \dots, N\}} \|\mathbf{r} - \mathbf{s}_i\|. \quad (1)$$

The BER can be used as the transmission performance measure. For AWGN channels with PSD equal to  $N_0/2$ , the conventional Symbol Error Rate (SER) expression based on the union bound estimate is [7]

$$\text{SER} \approx K_{\min} \mathcal{Q}\left(\frac{d_{\min}}{\sqrt{2N_0}}\right), \quad (2)$$

where  $d_{\min}$  is the distance between each nearest pair of signal points,  $K_{\min}$  is the average number of nearest neighbors, and  $\mathcal{Q}$  is the Complimentary Cumulative Distribution Function (CCDF) of the standard Gaussian random variable, i.e.,  $\mathcal{Q}(x) = \int_x^\infty \frac{1}{\sqrt{2\pi}} e^{-z^2/2} dz$ . With the bit rate equal to  $b$  bit/symbol, the BER can be approximated from the SER per bit using [7]

$$\text{BER} \approx \frac{1}{b} \times \text{SER} = \frac{K_{\min}}{b} \mathcal{Q}\left(\frac{d_{\min}}{\sqrt{2N_0}}\right). \quad (3)$$

In this work, each data symbol is mapped to one of many possible signal points. The set of signal points for each data symbol will be referred to as a cluster. In Table 1, the data symbol for bits 00 corresponds to the cluster  $\{(A, 0, 0, 0), (A, 0, A, 0), (0, A, A, A)\}$ , the data symbol for bits 01 corresponds to the cluster  $\{(0, A, 0, 0), (A, 0, 0, A), (A, 0, A, A)\}$ , and so on. Note that, at the receiver, an error between signal points in the same cluster does not lead to any bit error. Therefore, in evaluating the BER, the minimum inter-cluster distance instead of the minimum distance between signal points should be considered. Figure 5 illustrates the difference between the minimum inter-cluster distance and the minimum distance between signal points.

To adopt the minimum inter-cluster distance, the BER expression in (3) is modified to

$$\text{BER} \approx \frac{1}{b} \times \text{SER} = \frac{\tilde{K}_{\min}}{b} \mathcal{Q}\left(\frac{\tilde{d}_{\min}}{\sqrt{2N_0}}\right), \quad (4)$$

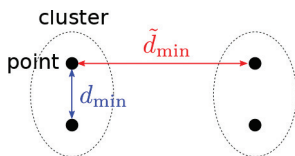


Figure 5: Minimum inter-cluster distance ( $\tilde{d}_{\min}$ ) vs. minimum distance between signal points ( $d_{\min}$ ).

where  $\tilde{d}_{\min}$  is the minimum inter-cluster distance and  $\tilde{K}_{\min}$  is the average number of nearest neighbors in different clusters.

As in [13], the BER will be considered in terms of the ratio  $A^2/N_0$ , which is an indicator of the channel quality. The next section considers using distinct modulation schemes for different dimming levels, for which the constellations in Table 1 provides one specific example.

### 3 Distinct Modulation Schemes for Different Dimming Levels

To provide for low, medium, and high illumination levels,  $M$ -PPM, multi-pulse  $M$ -PPM with  $K = M/2$ , and  $M$ -IPPM can be chosen as the modulation schemes, respectively. Given  $M$ , the three illumination levels are  $1/M \times 100\%$ ,  $50\%$ , and  $(M - 1)/M \times 100\%$ . For multi-pulse  $M$ -PPM with  $K = M/2$ , one simple choice of  $M$  signal points can be found based on using 2-PPM for one data bit at a time. Table 1 shows an example of this choice for  $M = 4$ .

For the constellations in Table 1, the signal points  $(A, 0, 0, 0)$  and  $(A, 0, 0, A)$  imply that  $\tilde{d}_{\min} = A$ . It is straightforward to verify by inspection that, for each signal point, the number of nearest neighbors in different clusters is (from top to bottom and from left to right) 1, 3, 2, 2, 3, 1, 1, 3, 2, 1, 3, and 2, respectively. It follows that the average is  $\tilde{K}_{\min} = 2$ . With  $b = 2$  bit/symbol, the corresponding BER expression in (4) is

$$\text{BER} \approx \mathcal{Q}\left(\sqrt{\frac{A^2}{2N_0}}\right). \quad (5)$$

More generally, the problem of selecting signal constellations for different dimming levels can be viewed as a binary code design problem. In particular, with  $M$  timeslots per symbol, each codeword contains  $M$  bits associated with the  $M$  timeslots. Each bit is equal to 1 when its timeslot contains a pulse, and is 0 otherwise. The constellation for each dimming level corresponds to a constant-weight code with a fixed Hamming weight. Note that a higher weight yields a higher illumination level. For example, the constellations in Table 1 correspond to codes with Hamming weights 1, 2, and 3, respectively. When

two codewords have the Hamming distance (i.e., number of bits that differ) equal to  $d_H$ , the distance between their corresponding signal points is  $\sqrt{d_H A}$ .

The constellation selection problem can be formulated as an ILP problem whose objective is to maximize the minimum inter-cluster distance between signal points, which is equivalent to maximizing the minimum inter-cluster Hamming distance between codewords. Let  $w_L, w_M, w_H$  denote the low, medium, and high target Hamming weights, respectively. These Hamming weights correspond to low, medium, and high illumination levels, respectively. The ILP formulation could be extended to accommodate more than three illumination levels, e.g., 5 Hamming weights for 5 illumination levels, in a straightforward fashion. Define the following input parameters for ILP.

- $N$ : number of candidate codewords with Hamming weight  $w_L$  or  $w_M$  or  $w_H$ , equal to  $\binom{M}{w_L} + \binom{M}{w_M} + \binom{M}{w_H}$
- $C$ : number of signal point clusters, equal to  $M$  (one for each data symbol)
- $L_n$ : equal to 1 if codeword  $n$  has Hamming weight  $w_L$ , and 0 otherwise
- $M_n$ : equal to 1 if codeword  $n$  has Hamming weight  $w_M$ , and 0 otherwise
- $H_n$ : equal to 1 if codeword  $n$  has Hamming weight  $w_H$ , and 0 otherwise
- $D_{nn'}$ : Hamming distance between codewords  $n$  and  $n'$

Decision variables of ILP are defined below.

- $x_{nc} \in \{0, 1\}$ : equal to 1 if codeword  $n$  is selected for cluster  $c$ , and 0 otherwise
- $y_{nn'} \in \{0, 1\}$ : equal to 1 if both codewords  $n$  and  $n'$  are selected
- $z \in \{1, 2, 3, \dots\}$ : equal to the minimum inter-cluster Hamming distance between the selected clusters of codewords.

For convenience, let  $\mathcal{N} = \{1, \dots, N\}$  and  $\mathcal{C} = \{1, \dots, C\}$ . The ILP problem for constellation selection is as follows.

$$\text{maximize } z \tag{6}$$

$$\text{subject to } \forall c \in \mathcal{C}, \sum_{n \in \mathcal{N}} L_n x_{nc} = 1 \tag{7}$$

$$\forall c \in \mathcal{C}, \sum_{n \in \mathcal{N}} M_n x_{nc} = 1 \tag{8}$$

$$\forall c \in \mathcal{C}, \sum_{n \in \mathcal{N}} H_n x_{nc} = 1 \quad (9)$$

$$\forall n, n' \in \mathcal{N} \text{ with } n \neq n', \forall c, c' \in \mathcal{C} \text{ with } c \neq c',$$

$$y_{nn'} \geq x_{nc} + x_{n'c'} - 1 \quad (10)$$

$$\forall n, n' \in \mathcal{N} \text{ with } n \neq n', \forall c, c' \in \mathcal{C} \text{ with } c \neq c',$$

$$z \leq D_{nn'} y_{nn'} + \text{Inf}(1 - y_{nn'}) \quad (11)$$

The objective in (6) is to maximize the minimum inter-cluster Hamming distance between the selected codewords. The constraints in (7), (8), and (9) ensure that exactly one codeword with each target Hamming weight is selected for each cluster. In (10), each  $y_{nn'}$  is forced to be 1 when codewords  $n$  and  $n'$  are selected to be in different clusters. Finally, in (11),  $z$  is kept no more than the Hamming distance between any pair of selected codewords in different clusters. In (11), ‘‘Inf’’ denotes a very large quantity, e.g., the maximum possible number of the programming environment. Note that the constraint is automatically satisfied when  $y_{nn'} = 0$ .

While the above ILP problem can be solved using a software tool, e.g., Python [19] with the PuLP library [18] as previously used in [20], the ILP approach has the following drawbacks. First, the computational complexity in solving the ILP problem is high, especially for large  $M$ . In particular, the complexity depends on the number of integer variables, which in the above ILP problem is dominated by the variables of the form  $y_{nn'}$ . For  $M$ -bit codewords with Hamming weights  $M/4$ ,  $M/2$ , and  $3M/4$ , the number of candidate codewords is  $\binom{M}{M/4} + \binom{M}{M/2} + \binom{M}{3M/4}$ , yielding the number of  $y_{nn'}$ 's equal to  $[\binom{M}{M/4} + \binom{M}{M/2} + \binom{M}{3M/4}]^2$ . For  $M = 4, 8, 16$ , this number is equal to 196, 15876,  $2.78 \times 10^8$ , respectively. It can be seen that the number of integer variables grows quite quickly with  $M$ .

In addition to high computational complexity in solving the ILP problem, after codewords are obtained, the coding and decoding complexities involved in the associated table lookup process are high. In the next section, an alternative dimming approach without these drawbacks is proposed based on time division between  $M$ -PPM and  $M$ -IPPM.

## 4 Dimming Using Time Division between $M$ -PPM and $M$ -IPPM

### 4.1 Time-Division $M$ -PPM/ $M$ -IPPM Signals

In this section, time division between  $M$ -PPM and  $M$ -IPPM is proposed to provide flexible dimming in VLC. More specifically, each of  $M$  data symbols is assigned a cluster of two signal points, one from  $M$ -PPM and its corresponding signal point from  $M$ -IPPM. Table 1 without the multi-pulse PPM constellation

provides an example for  $M = 4$ . In particular, the cluster associated with the symbol for data bits 00 is  $\{(A, 0, 0, 0), (0, A, A, A)\}$ , the cluster associated with data bits 01 is  $\{(0, A, 0, 0), (A, 0, A, A)\}$ , and so on.

Let  $\alpha$  and  $1 - \alpha$  be the fractions of time in which  $M$ -IPPM and  $M$ -PPM are used, respectively. The corresponding illumination is the weighted sum of the illumination levels of  $M$ -PPM and  $M$ -IPPM, which is equal to

$$\left( (1 - \alpha) \frac{1}{M} + \alpha \frac{M - 1}{M} \right) \times 100\%. \quad (12)$$

In principle, by varying  $\alpha$  from 0 to 1, any illumination level from  $1/M \times 100\%$  to  $(M - 1)/M \times 100\%$  can be obtained, and is independent of data bits. However, in practice,  $\alpha$  can be selected from a finite set of values, e.g.,  $\alpha \in \{0, 0.25, 0.5, 0.75, 1\}$  for 5 dimming levels. Figure 6 illustrates data signals for 5 different values of  $\alpha$  for the case of  $M = 4$ .

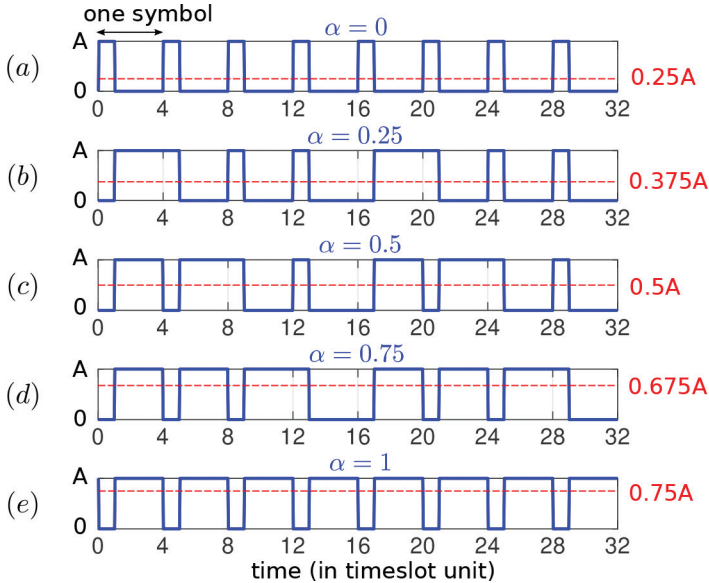


Figure 6: Example time-division 4-PPM/4-IPPM signals for (a)  $\alpha = 0$ , (b)  $\alpha = 0.25$ , (c)  $\alpha = 0.5$ , (d)  $\alpha = 0.75$ , and (e)  $\alpha = 1$ , with the average signal values shown as red dashed lines. Each example signal repeatedly transmits symbols for bits 00.

The choice of  $M$  provides a trade-off between the data rate and the supported dimming range, as illustrated in Figure 7. More specifically, as shown in Figure 7(a), the data rate, which is equal to  $(\log_2 M)/M$  bit/timeslot, decreases as  $M$  increases. Figure 7(b) shows that the minimum illumination level (equal to  $1/M \times 100\%$  of maximum illumination) decreases with  $M$  while

the maximum illumination level (equal to  $(M - 1)/M \times 100\%$ ) increases with  $M$ . Finally, Figure 7(c) shows that, as we increase  $M$ , the data rate decreases while the dimming range, which is the difference between the maximum and minimum illumination levels and is equal to  $(M - 2)/M \times 100\%$ , increases. Therefore, the choice of  $M$  should balance between the data rate and the dimming range.

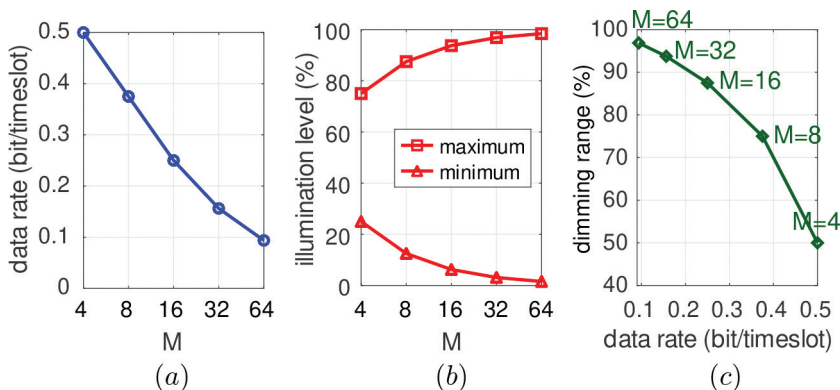


Figure 7: (a) data rate (in bit/timeslot) vs.  $M$ , (b) dimming level (in % of maximum illumination) vs.  $M$ , and (c) dimming range (in %) vs. data rate for time-division  $M$ -PPM/ $M$ -IPPM.

#### 4.2 BER Performance of Time-Division $M$ -PPM/ $M$ -IPPM

Besides the flexibility in setting a dimming level, compared to using distinct modulation schemes for different dimming levels, the time division approach may also improve the BER performance. In the case of  $M = 4$ , using time division between 4-PPM and 4-IPPM results in a combined constellation with 8 signal points (in top and bottom rows of Table 1) instead of 12 signal points (in all rows of Table 1). By inspection, the minimum inter-cluster distance is  $\sqrt{2}A$ . Each  $M$ -PPM signal point has 3 nearest neighbors in the  $M$ -PPM constellation, and 3 more nearest neighbors in the  $M$ -IPPM constellation. These nearest neighbors are all in different clusters. Consequently,  $\tilde{d}_{\min} = \sqrt{2}A$  and  $\tilde{K}_{\min} = 6$ . With  $b = 2$  bit/symbol, the BER expression in (4) becomes

$$\text{BER} \approx 3Q\left(\sqrt{\frac{A^2}{N_0}}\right). \quad (13)$$

As shown in Figure 8, the BER in (13) is an improvement compared with the value in (5) mainly due to a larger value of  $\tilde{d}_{\min}$  ( $\sqrt{2}A$  instead of  $A$ ).

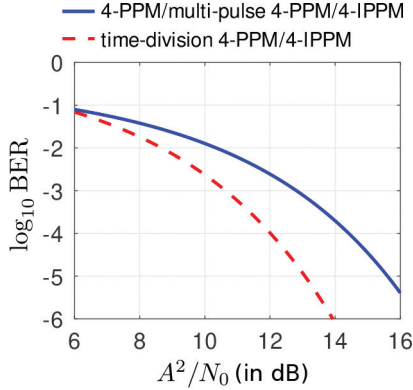


Figure 8: BER comparison between using separate 4-PPM/multi-pulse 4-PPM/4-IPPM constellations for different dimming levels and using time-division 4-PPM/4-IPPM.

To compare the BER performances with the same transmit optical powers among different modulation schemes, Figure 9 shows the BERs for different transmit optical powers. It is assumed without loss of generality that the constant signal  $A = 1$  corresponds to the average power of 1 W (30 dBm). In addition, the value of  $N_0$  is fixed such that the ratio  $A^2/N_0$  is equal to 15 dB for  $A = 1$ . For clear comparisons, BERs are compared separately for each illumination level. For 25% illumination using either 4-PPM or time-division 4-PPM/4-IPPM with  $\alpha = 0$ , the average transmit optical power is  $A/4$ . For 50% illumination using either multi-pulse PPM with  $K = M/2$  or time-division 4-PPM/4-IPPM with  $\alpha = 0.5$ , the power is  $A/2$ . For 75% illumination using either 4-IPPM or time-division 4-PPM/4-IPPM with  $\alpha = 1$ , the power is  $3A/4$ .

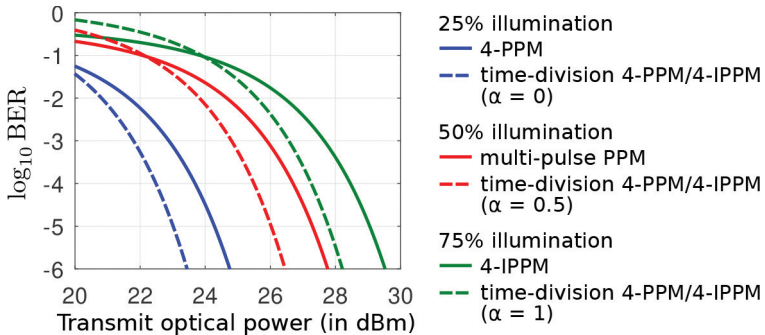


Figure 9: BER comparison at 25%, 50%, and 75% illumination levels for different transmit optical powers.

It can be seen from Figure 9 that, for each illumination level, the proposed time-division approach provides in general better performances compared to using a separate modulation scheme. For example, around a BER target of  $10^{-4}$ , the proposed scheme requires lower optical powers at all illumination levels. Figure 9 also shows the effects of increasing the dimming parameter  $\alpha$  with respect to the BER performance. It can be seen that, for the same BER target, e.g.,  $10^{-4}$ , increasing  $\alpha$  for a higher illumination level leads to a higher transmit optical power requirement.

At high BERs (above  $10^{-1}$ ), the BERs from time-division 4-PPM/4-IPPM, i.e.,  $3Q(\sqrt{A^2/N_0})$  from (13), can be higher than the BERs from using a separate modulation scheme for each dimming level, i.e.,  $Q(\sqrt{A^2/2N_0})$  from (5). This is due to the multiplicative factor of 3 from a higher number of nearest-neighbor signal points for time-division 4-PPM/4-IPPM. However, at low BERs, lower probability values from the  $Q$  function (from a higher minimum distance between signal points) offsets the multiplicative factor of 3, making the BERs lower for time-division 4-PPM/4-IPPM. The two BER expressions are equal when  $\sqrt{A^2/N_0} \approx 1.86$  since  $3Q(1.86) \approx Q(1.86/\sqrt{2})$ . With  $N_0 \approx 0.0316$  fixed from the above assumption (with  $A$  varying) that  $A^2/N_0 = 15$  dB when  $A = 1$ , the two BER expressions are equal for  $A \approx 0.331$ . The corresponding transmit optical powers for 25%, 50%, and 75% illumination levels (i.e.,  $A/4$ ,  $A/2$ , and  $3A/4$ ) are approximately 19.2, 22.2, and 23.9 dBm. Hence, the three pairs of BER plots in Figure 9 intersect at these values of transmit optical powers.

For  $M \in \{8, 16, \dots\}$ , the proposed approach yield a combined constellation containing  $2M$  signal points, with  $M$  points from  $M$ -PPM and  $M$  points from  $M$ -IPPM. Each point from  $M$ -PPM and its corresponding point in  $M$ -IPPM form a cluster, e.g.,  $(A, 0, 0, 0, 0, 0, 0, 0)$  and  $(0, A, A, A, A, A, A, A)$  for data bits 000 in case of  $M = 8$ . It can be observed that the distance between any signal point in  $M$ -PPM and any point in  $M$ -IPPM is at least  $\sqrt{(M-2)A}$  since there are  $M-1$  pulses for any  $M$ -IPPM symbol and 1 pulse for any  $M$ -PPM symbol, yielding at least  $(M-1) - 1 = M-2$  timeslots that are different. For  $M > 4$ , this distance  $\sqrt{(M-2)A}$  is greater than  $\sqrt{2}A$ , which is the distance between any two signal points within  $M$ -PPM, and between any two signal points within  $M$ -IPPM. It follows that, for  $M > 4$ ,  $\tilde{d}_{\min} = \sqrt{2}A$  and  $\tilde{K}_{\min} = M-1$ .

In summary, the BER approximation in (4) for time-division  $M$ -PPM/ $M$ -IPPM can be expressed below.

$$\text{BER} \approx \begin{cases} 3Q\left(\sqrt{\frac{A^2}{N_0}}\right), & M = 4 \\ \frac{M-1}{\log_2 M} Q\left(\sqrt{\frac{A^2}{N_0}}\right), & M \in \{8, 16, \dots\} \end{cases} \quad (14)$$

Since  $\tilde{d}_{\min} = \sqrt{2}A$  in all cases, the BER performance of the proposed time-division approach is approximately the same as in the case of  $M$ -PPM or  $M$ -IPPM with the modulation scheme known. Essentially, compared with data transmissions without dimming support, there is no BER degradation from using the proposed dimming approach.

### 4.3 Decision Rule for Minimum-Distance Detection

This section presents the specific decision rule associated with the minimum-distance detection of data bits for the proposed time-division  $M$ -PPM/ $M$ -IPPM scheme. Starting from the minimum-distance decision rule in (1), note that minimizing the distance  $\|\mathbf{r} - \mathbf{s}_i\|$  is equivalent to minimizing the squared distance, yielding

$$i^* = \arg \min_{i \in \{1, \dots, N\}} \|\mathbf{r} - \mathbf{s}_i\|^2. \quad (15)$$

Expanding the squared distance term  $\|\mathbf{r} - \mathbf{s}_i\|^2$ , the decision rule can be rewritten as

$$\begin{aligned} i^* &= \arg \min_{i \in \{1, \dots, N\}} \|\mathbf{r} - \mathbf{s}_i\|^2 \\ &= \arg \min_{i \in \{1, \dots, N\}} \|\mathbf{r}\|^2 + \|\mathbf{s}_i\|^2 - 2\mathbf{r}^\top \mathbf{s}_i \\ &= \arg \min_{i \in \{1, \dots, N\}} \|\mathbf{s}_i\|^2 - 2\mathbf{r}^\top \mathbf{s}_i, \end{aligned} \quad (16)$$

where  $\mathbf{r}^\top$  denotes the transpose of vector  $\mathbf{r}$  and the last equality follows from dropping the term  $\|\mathbf{r}\|^2$  that does not depend on  $i$ .

Arrange the  $M$  signal points from  $M$ -PPM as  $\mathbf{s}_1, \dots, \mathbf{s}_M$  and their associated signal points from  $M$ -IPPM as  $\mathbf{s}_{M+1}, \dots, \mathbf{s}_{2M}$ . For example, for  $M = 4$ , the signal points are as shown below, where each row corresponds to a cluster of 2 signal points.

$$\begin{aligned} \text{Data bits } 00 : \mathbf{s}_1 &= (A, 0, 0, 0), \quad \mathbf{s}_5 = (0, A, A, A) \\ \text{Data bits } 01 : \mathbf{s}_2 &= (0, A, 0, 0), \quad \mathbf{s}_6 = (A, 0, A, A) \\ \text{Data bits } 10 : \mathbf{s}_3 &= (0, 0, A, 0), \quad \mathbf{s}_7 = (A, A, 0, A) \\ \text{Data bits } 11 : \mathbf{s}_4 &= (0, 0, 0, A), \quad \mathbf{s}_8 = (A, A, A, 0) \end{aligned} \quad (17)$$

With the above signal point arrangement, the decision rule for a signal cluster (instead of a signal point) of a data symbol becomes

$$\begin{aligned} i^* &= \arg \min_{i \in \{1, \dots, M\}} \min \left( \|\mathbf{s}_i\|^2 - 2\mathbf{r}^\top \mathbf{s}_i, \|\mathbf{s}_{M+i}\|^2 - 2\mathbf{r}^\top \mathbf{s}_{M+i} \right) \\ &= \arg \min_{i \in \{1, \dots, M\}} \min \left( A^2 - 2Ar_i, (M-1)A^2 - 2A(R - r_i) \right), \end{aligned} \quad (18)$$

where  $R = \sum_{i=1}^M r_i$ . The rule can be simplified to

$$\begin{aligned} i^* &= \arg \min_{i \in \{1, \dots, M\}} \min \left( -2Ar_i, (M-2)A^2 - 2A(R-r_i) \right) \\ &= \arg \max_{i \in \{1, \dots, M\}} \max \left( r_i, R - r_i - \frac{M-2}{2}A \right). \end{aligned} \quad (19)$$

Figure 10 shows BER values obtained from the expression in (14) and from simulation experiments using the decision rule in (19). Simulation programs were developed using the Octave software [9] on the Ubuntu 22.04.2 LTS operating system and the simulation parameters as given in Table 2. A close match between analytical and simulation results can be observed.

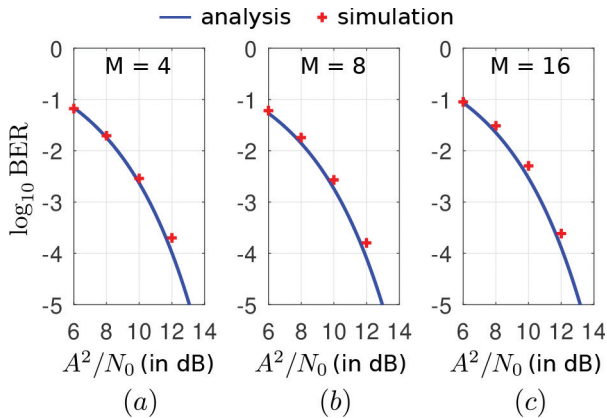


Figure 10: BER values from the BER expression in (14) and from simulation experiments using the decision rule in (19) for (a)  $M = 4$ , (b)  $M = 8$ , and (c)  $M = 16$ .

Table 2: Simulation parameters for BER evaluation.

Simulation parameter	Value
Number of transmitted symbols	$10^5$
$M$ for time-division $M$ -PPM/ $M$ -IPPM	4, 8, 16
Dimming parameter ( $\alpha$ )	0.25
Pulse amplitude $A$	1
Ratio $A^2/N_0$	6–14 dB

Comparing the decision rule in (19) and the rules for  $M$ -PPM ( $i^* = \arg \max_{i \in \{1, \dots, M\}} r_i$ ) and for  $M$ -IPPM ( $i^* = \arg \min_{i \in \{1, \dots, M\}} r_i$ ), it can be seen that

these rules are based on the same set of values  $r_1, \dots, r_M$ . Hence, the proposed time-division  $M$ -PPM/ $M$ -IPPM scheme does not increase the hardware complexity. Regarding the computational complexity, which reflects the demodulation latency, the decision rule in (19) involves finding the maximum out of  $2M$  values while the rules for  $M$ -PPM and for  $M$ -IPPM involve finding the maximum out of  $M$  values. Hence, the computational complexity of the proposed scheme is twice as high compared to using  $M$ -PPM or  $M$ -IPPM. In terms of the order notation, all schemes have the computational complexity of  $O(M)$ .

## 5 Detection of Successive Symbols for BER Improvement

In the application scenario considered in this work, each LED lamp repeatedly transmits a location number. Therefore, it is possible to utilize successive transmitted symbols for BER improvement. More specifically, each data symbol is repeatedly transmitted, possibly with some separations by some other data symbols. This section considers symbol detection based on two successive transmissions of the same symbol. Note that, based the proposed flexible dimming using time-division  $M$ -PPM/ $M$ -IPPM, two successive symbols may be transmitted using different modulation schemes.

Let  $\mathbf{r}_1 = (r_1, \dots, r_M)$  and  $\mathbf{r}_2 = (r_{M+1}, \dots, r_{2M})$  contain  $M$  received signal values for symbol 1 and symbol 2, respectively. Recall that, for detection based on a single transmitted symbol, symbol  $i$  is associated with the cluster of 2 signal points, which is  $\mathcal{C}_i = \{\mathbf{s}_i, \mathbf{s}_{M+i}\}$ . For detection based on 2 symbols whose modulation schemes may differ, symbol  $i$  is associated with the cluster of 4 signal points below.

$$\mathcal{C}_i = \left\{ (\mathbf{s}_i, \mathbf{s}_i), (\mathbf{s}_i, \mathbf{s}_{M+i}), (\mathbf{s}_{M+i}, \mathbf{s}_i), (\mathbf{s}_{M+i}, \mathbf{s}_{M+i}) \right\} \quad (20)$$

The values of  $\tilde{d}_{\min}$  and  $\tilde{K}_{\min}$  are next identified.

Recall that, for single-symbol detection,  $\tilde{d}_{\min} = \sqrt{2}A$ . With two-symbol detection,  $\tilde{d}_{\min} = 2A$  and is between the same nearest inter-cluster neighbors. As a specific example, for  $M = 4$ , the signal points  $(A, 0, 0, 0)$  and  $(0, A, 0, 0)$  are nearest inter-cluster neighbors at the distance  $\sqrt{2}A$ . When two-symbol detection is considered, the signal points  $(A, 0, 0, 0, A, 0, 0, 0)$  and  $(0, A, 0, 0, 0, A, 0, 0)$  are nearest inter-cluster neighbors at the distance  $2A$ .

For  $\tilde{K}_{\min}$ , consider two separate cases:  $M = 4$  and  $M \in \{8, 16, \dots\}$ . For  $M = 4$ , in single-symbol detection, each signal point has 6 nearest inter-cluster neighbors. In fact, all signal points in different clusters are nearest neighbors. For two-symbol detection, extensions of the same 6 nearest neighbors with possibly two different modulation schemes in the second symbol give rise to 12 nearest neighbors (6 from extensions using the same modulation scheme and 6 from extensions using the other scheme). Therefore,  $\tilde{K}_{\min} = 12$  for  $M = 4$ .

For  $M \in \{8, 16, \dots\}$ , each signal point has  $M - 1$  inter-cluster nearest neighbors from the same constellation. With two-symbol detection, extensions of the same  $M - 1$  nearest neighbors with the same modulation scheme give rise to  $M - 1$  nearest neighbors. Note that having the second symbol with a different modulation scheme increases the distance beyond  $\tilde{d}_{\min}$ . Therefore,  $\tilde{K}_{\min} = M - 1$  for  $M \in \{8, 16, \dots\}$ .

In summary, using two-symbol detection, the BER expression in (21) becomes

$$\text{BER} \approx \begin{cases} 6\mathcal{Q}\left(\sqrt{\frac{2A^2}{N_0}}\right), & M = 4 \\ \frac{M-1}{\log_2 M} \mathcal{Q}\left(\sqrt{\frac{2A^2}{N_0}}\right), & M \in \{8, 16, \dots\} \end{cases}. \quad (21)$$

Figure 11 shows numerical BER values from single-symbol detection in (14) and from two-symbol detection in (21) for the proposed time-division  $M$ -PPM/ $M$ -IPPM scheme. Significant BER improvements from two-symbol detection can be observed. The improvements are mainly due to the increase in  $\tilde{d}_{\min}$  ( $2A$  instead of  $\sqrt{2}A$ ).

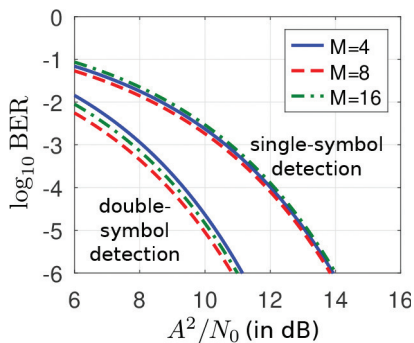


Figure 11: BER comparison between using single-symbol detection and two-symbol detection for time-division  $M$ -PPM/ $M$ -IPPM.

Based on the signal point clusters in (20), the decision rule for minimum-distance detection in (16) can be expressed as

$$i^* = \arg \min_{i \in \{1, \dots, M\}} \min \left( \|\mathbf{s}_i\|^2 - 2\mathbf{r}_1^T \mathbf{s}_i + \|\mathbf{s}_i\|^2 - 2\mathbf{r}_2^T \mathbf{s}_i, \right. \\ \|\mathbf{s}_i\|^2 - 2\mathbf{r}_1^T \mathbf{s}_i + \|\mathbf{s}_{M+i}\|^2 - 2\mathbf{r}_2^T \mathbf{s}_{M+i}, \\ \|\mathbf{s}_{M+i}\|^2 - 2\mathbf{r}_1^T \mathbf{s}_{M+i} + \|\mathbf{s}_i\|^2 - 2\mathbf{r}_2^T \mathbf{s}_i, \\ \left. \|\mathbf{s}_{M+i}\|^2 - 2\mathbf{r}_1^T \mathbf{s}_{M+i} + \|\mathbf{s}_{M+i}\|^2 - 2\mathbf{r}_2^T \mathbf{s}_{M+i} \right)$$

$$\begin{aligned}
&= \arg \min_{i \in \{1, \dots, M\}} \min \left( A^2 - 2Ar_i + A^2 - 2Ar_{M+i}, \right. \\
&\quad A^2 - 2Ar_i + (M-1)A^2 - 2A(R_2 - r_{M+i}), \\
&\quad (M-1)A^2 - 2A(R_1 - r_i) + A^2 - 2Ar_{M+i}, \\
&\quad \left. (M-1)A^2 - 2A(R_1 - r_i) + (M-1)A^2 - 2A(R_2 - r_{M+i}) \right), \quad (22)
\end{aligned}$$

where  $R_1 = \sum_{i=1}^M r_i$  and  $R_2 = \sum_{i=M+1}^{2M} r_i$ . The decision rule in (22) can be simplified to

$$\begin{aligned}
i^* = \arg \max_{i \in \{1, \dots, M\}} \max \left( r_i + r_{M+i}, \right. \\
\quad r_i + (R_2 - r_{M+i}) - \frac{M-2}{2}A, \\
\quad (R_1 - r_i) + r_{M+i} - \frac{M-2}{2}A, \\
\quad \left. (R_1 - r_i) + (R_2 - r_{M+i}) - (M-2)A \right). \quad (23)
\end{aligned}$$

Figure 12 shows BER values obtained from the expression in (21) and from simulation experiments based on 100,000 transmitted data symbols with  $\alpha = 0.25$  and using the decision rule in (23). A close match between analytical and simulation results can be observed.

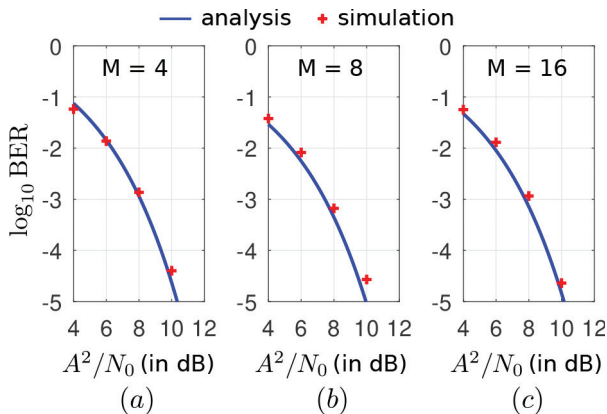


Figure 12: BER values from the BER expression in (21) and from simulation experiments using the decision rule in (23) for (a)  $M = 4$ , (b)  $M = 8$ , and (c)  $M = 16$ .

While the main purpose of detection based on the decision rule in (23) is to obtain transmitted data symbols, the process can be used for joint detection of modulation schemes and data symbols. In particular, with respect to  $i^*$ , the position of the inner maximization in (23) indicates the modulation formats

used. For inner maximum positions 1 to 4, the modulation formats are (1)  $M$ -PPM followed by  $M$ -PPM, (2)  $M$ -PPM followed by  $M$ -IPPM, (3)  $M$ -IPPM followed by  $M$ -PPM, and (4)  $M$ -IPPM followed by  $M$ -IPPM, respectively. However, as long as data symbols are retrieved, the knowledge of modulation schemes used is in general not required.

## 6 Conclusion

In this work, a flexible dimming technique for PPM based data transmissions in indoor VLC systems was proposed and analyzed. By representing each data symbol using a cluster of signal points chosen from multiple constellations instead of one signal point from one constellation, a data symbol can be transmitted with the dimming level determined by the chosen signal point from its cluster. For flexibility, dimming levels at different LED transmitters may differ, and the receiver may move from one location to another without knowing the dimming levels. Based on time division between  $M$ -PPM and  $M$ -IPPM, a range of dimming levels between  $1/M \times 100\%$  and  $(M - 1)/M \times 100\%$  of the maximum illumination level can be supported. The associated BER performance analysis was provided, where the BER is based on the minimum inter-cluster distance instead of the minimum distance between signal points as used in the conventional analysis. Compared to using different modulation schemes for different dimming levels, using time-division  $M$ -PPM/ $M$ -IPPM provides more choices of dimming levels with equal or better BER performances. Finally, for BER improvement, detection of successive data symbols was proposed and analyzed.

## Biographies

**Poompat Saengudomlert** obtained the B.S.E. degree in Electrical Engineering from Princeton University, USA, in 1996. He then obtained the S.M. and Ph.D. degrees, both in Electrical Engineering and Computer Science, from Massachusetts Institute of Technology (MIT), USA, in 1998 and 2002 respectively. From 2003 to 2004, he was a Postdoctoral Research Associate in Laboratory of Information and Decision Systems (LIDS) at MIT. From 2005 to early 2013, he was a faculty member (Lecturer, Assistant Professor, and finally Associate Professor) in Telecommunications at Asian Institute of Technology (AIT), Thailand. From May 2013 up to present, he is a Research Scholar and Associate Professor in Telecommunication Engineering at Bangkok University's Center of Research in Optoelectronics, Communication and Computational Systems (BU-CROCCS), Thailand. His research interest includes visible light communications, communication theory, and network optimization.

**Karel L. Sterckx** received a Master of Applied Engineering in Electrical and Electronic Engineering from a college that is currently part of Catholic University Leuven (Belgium) in 1986. In 1997, he obtained a Master of Science in Optoelectronics and Communications Systems from Northumbria University (UK) and, in 2000, a Ph.D. from Swansea University (UK) for work on infrared wireless communication links. He has experience as a practicing engineer in the Belgian audio-visual industry, and has been lecturing at colleges and universities in Thailand since 1993. He has been a resident of Thailand for over 20 years and joined Bangkok University in 2010 as Research Scholar. Since 2012, he is the director of the Bangkok University Center of Research in Optoelectronics, Communications and Computational Systems (BU-CROCCS). His research efforts concentrate on broadband indoor Optical Wireless Communication and Software Defined Communication Systems.

## References

- [1] J. Armstrong, Y. A. Sekercioglu, and A. Neild, “Visible light positioning: A roadmap for international standardization,” *IEEE Communications Magazine*, 51(12), 2013, 2013, 68–73.
- [2] A. E. Brouwer, J. B. Shearer, N. J. A. Sloane, and W. D. Smith, “A new table of constant weight codes,” *IEEE Transactions on Information Theory*, 36(6), 1990, 1990, 1334–80.
- [3] N. Chi, *LED-Based Visible Light Communications*, Springer, 2018, 2018.
- [4] S. Das and S. K. Mandal, “Dimming controlled multi header hybrid PPM (MH-HPPM) for visible light communication,” *Optical and Quantum Electronics*, 53(2), 2021, 2021.
- [5] T.-H. Do and M. Yoo, “An in-depth survey of visible light communication based positioning systems,” *Sensors*, 16(5), 2016, 2016.
- [6] F. Fang, S. Xiao, Z. Chen, and W. Hu, “Shaped polar codes for dimmable visible light communication,” *Optics Communications*, 496, 2021, 2021.
- [7] G. D. Forney and G. Ungerboeck, “Modulation and coding for linear Gaussian channels,” *IEEE Transactions on Information Theory*, 44(6), 1998, 1998, 2384–415.
- [8] Z. Ghassemlooy, W. Popoola, and S. Rajbhandari, *Optical Wireless Communications: System and Channel Modelling with MATLAB, Second Edition*, CRC Press, 2019, 2019.
- [9] GNU, “GNU Octave: Scientific Programming Language,” [octave.org/index.html](https://octave.org/index.html), 2023.
- [10] IEEE, “IEEE Standard for Local and Metropolitan Area Networks—Part 15.7: Short-Range Optical Wireless Communications,” *IEEE Standard 802.15.17–2018*, 2018, 2018.

- [11] B. W. Kim and S.-Y. Jung, “Dimmable spatial intensity modulation for visible-light communication: Capacity analysis and practical design,” *Current Optics and Photonics*, 2(6), 2018, 2018, 532–9.
- [12] H.-C. Kim, S.-S. Lee, and S.-Y. Jung, “Dimmable VLC demonstration systems based on LED,” *Proceedings of SPIE: Infrared, Millimeter-Wave, and Terahertz Technologies II*, 2012, 2012.
- [13] R. Lee, K. Yun, J.-H. Yoo, S.-Y. Jung, and J. K. Kwon, “Performance analysis of  $M$ -ary PPM in dimmable visible light communications,” *Proceedings of International Conference on Ubiquitous and Future Networks (ICUFN)*, 2013, 2013, 2384–415.
- [14] S. H. Lee, S.-Y. Jung, and J. K. Kwon, “Modulation and coding for dimmable visible light communication,” *IEEE Communications Magazine*, 53(2), 2015, 2015, 136–42.
- [15] G. A. Mapunda, R. Ramogomana, L. Marata, B. Basutli, A. S. Khan, and J. M. Chuma, “Indoor Visible light communication: A tutorial and survey,” *Wireless Communications and Mobile Computing*, 2020, 2020.
- [16] L. E. M. Matheus, A. B. Vieira, L. F. M. Vieira, M. A. M. Vieira, and O. Gnawali, “Visible light communication: Concepts, applications and challenges,” *IEEE Communications Surveys & Tutorials*, 21(4), 2019, 2019, 3204–37.
- [17] J. Noh, S. Lee, J. Kim, M. Ju, and Y. Park, “A dimming controllable VPPM-based VLC system and its implementation,” *Optics Communications*, 343, 2015, 2015, 34–7.
- [18] PuLP, “PuLP library for Python,” [pypi.org/project/PuLP](https://pypi.org/project/PuLP/), 2023.
- [19] Python, “Python software,” [www.python.org](https://www.python.org/), 2023.
- [20] P. Saengudomlert and K. L. Sterckx, “Automatic detection of dimmable pulse position modulation for visible light communication,” *Proceedings of the Asia Pacific Signal and Information Processing Association Annual Summit and Conference (APSIPA ASC)*, 2022, 2022.
- [21] K. L. Sterckx and P. Saengudomlert, “Visible light communications via dimmable LED lamps,” *Proceedings of the 16th European Conference on Networks and Optical Communications (NOC)*, 2011, 2011.
- [22] Y. Suh, C.-H. Ahn, and J. K. Kwon, “Dual-codeword allocation scheme for dimmable visible light communications,” *IEEE Photonics Technology Letters*, 25(13), 2013, 2013, 1274–7.
- [23] B. A. Vijayalakshmi and M. Nesasudha, “Flicker mitigation in dimmed LEDs installed indoors using vDSM digital technique under visible light communication,” *Optical and Quantum Electronics*, 52(2), 2020, 2020.
- [24] T. Wang, F. Yang, J. Song, and Z. Han, “Dimming techniques for visible light communications for human-centric illumination networks: State-of-the-art, challenges, and trends,” *IEEE Wireless Communications*, 27(4), 2020, 2020, 88–95.

- [25] F. Zafar, D. Karunatilaka, and R. Parthiban, “Dimming schemes for visible light communication: The state of research,” *IEEE Wireless Communications*, 22(2), 2015, 2015, 29–35.